

## Graphene on Ni(111): Strong interaction and weak adsorption

F. Mittendorfer,<sup>1,\*</sup> A. Garhofer,<sup>1</sup> J. Redinger,<sup>1</sup> J. Klimeš,<sup>2</sup> J. Harl,<sup>3</sup> and G. Kresse<sup>3</sup>

<sup>1</sup>*Institute of Applied Physics, TU Vienna, and Center for Computational Materials Science, Gusshausstrasse 25/134, A-1040 Wien, Austria*

<sup>2</sup>*Thomas Young Centre, London Centre for Nanotechnology and Department of Chemistry, University College London, London WC1E 6BT, United Kingdom*

<sup>3</sup>*Faculty of Physics, Universität Wien, and Center for Computational Materials Science, Sensengasse 8/12, A-1090 Wien, Austria*

(Received 9 November 2011; published 21 November 2011)

The adsorption of graphene on Ni(111) has been investigated on the basis of the adiabatic-connection fluctuation-dissipation theorem in the random phase approximation (RPA). Although we find a significant hybridization between the graphene  $\pi$  orbitals and Ni  $d_{z^2}$  states at a binding distance of 2.17 Å, the adsorption energy is still in the range of a typical physisorption (67 meV per carbon). An important contribution to the energy is related to a decrease in the exchange energy resulting from the adsorption-induced lower symmetry in the graphene layer. The energetics can be well reproduced using the computationally significantly cheaper van der Waals density functional theory with an appropriately chosen exchange-correlation functional.

DOI: 10.1103/PhysRevB.84.201401

PACS number(s): 81.05.ue, 75.75.-c, 85.75.-d

The discovery of the exceptional electronic properties of graphene, such as the linear band dispersion in the vicinity of the Dirac point,<sup>1</sup> has resulted in a surge of investigations in this field. Especially, the nearly ideal transport properties of graphene and the tunability of the charge carrier concentration by the ambipolar field effect<sup>2</sup> have led to a wide range of proposed applications for graphene-based electronics.<sup>3</sup> In addition, graphene supported on ferromagnetic materials, such as nickel, has been proposed as a promising path for the design of the spin-filtering devices needed for spintronics.<sup>4</sup>

Yet, on a fundamental level the interaction of graphene with a metallic surface is not well understood.<sup>5</sup> From an experimental point of view, this interaction has either been classified as a “weak” interaction [e.g., on Pt(111)],<sup>6</sup> where angle-resolved photoemission (ARPES) data show a merely shifted band crossing of the graphene  $\pi$  bands at the Dirac ( $K$ ) point, or a “strong” interaction (Ni, Co), where a pronounced splitting of the  $\pi$  states is observed.<sup>7</sup> In the case of graphene/Ni(111), the ARPES data display several peaks at the Dirac point at binding energies ranging from 0.7 to 2.65 eV, indicating a significant gap. Consequently, the splitting has been related to a strong hybridization induced by chemisorption of the graphene sheet. An overview on the experimental data can be found in a recent review.<sup>8</sup> The adsorption of graphene on Ni(111) is an especially suitable model system to scrutinize these interactions, as the small lattice mismatch between graphene and the Ni surface leads to epitaxial growth, keeping additional strain-induced contributions small.

From a theoretical point of view, the system is difficult to treat as both an accurate description of the metallic surface and the nonlocal correlation effects is needed. Several authors have investigated this system with standard density functional theory (DFT) approaches,<sup>9–12</sup> where the van der Waals (vdW) contributions are completely neglected. While the gradient-corrected [generalized gradient approximation (GGA)] exchange-correlation functionals yield too repulsive energy-distance curves, the local density approximation (LDA) yields an artificial minimum with completely wrong long-range asymptotic behavior. Furthermore, even the recently proposed van der Waals DFT (vdW-DF)<sup>13</sup> fails

to predict an appropriate structure for the graphene-metal interfaces. In a recent paper, Hamada and Otani showed that the originally proposed vdW functionals (vdW-DF, vdW-DF2) lead to no binding at all.<sup>14</sup> Although the use of vdW-DF with less repulsive exchange functionals leads to more reasonable results, the wide spread of the computed adsorption energies using different functionals underlines the need for a reference calculation.

It has recently been shown that an explicit evaluation of the correlation energy in the framework of the adiabatic-connection fluctuation-dissipation theorem (AC-FDT) in the random phase approximation (RPA) leads to a natural inclusion of the nonlocal van der Waals contributions,<sup>15</sup> is very systematic for noncovalent interactions,<sup>16</sup> offers an excellent description of the binding energy of graphite,<sup>17</sup> and yields an improved adsorption energy for molecules on metallic surfaces.<sup>18</sup> Here, we present RPA calculations to evaluate the delicate interplay between chemisorption and physisorption, determining the interaction of graphene with the ferromagnetic Ni(111) surface. We also discuss the effect of many-body ( $GW$ ) contributions on the band structure of graphene on Ni, and present an efficient method to treat much larger systems.

Our calculations were performed with the Vienna *ab initio* simulation package (VASP)<sup>19,20</sup> using the projector augmented-wave method.<sup>21</sup> Since the Ni 3s and 3p electrons are fairly polarizable, we found it necessary to include them in the correlation energy, increasing the adsorption energy at small graphene Ni distances. All calculations were performed at an RPA Ni lattice constant of 3.526 Å, which is very close to the experimental value of 3.524 Å. The Brillouin zone integration was done on a  $19 \times 19 \times 1$   $k$ -point mesh. The Ni(111) surface was modelled by a slab consisting of five layers and a vacuum width of  $\sim 14$  Å thickness. Further technical details can be found in Refs. 18 and 22.

Figure 1 shows the energy distance curves for graphene on Ni(111) using semilocal density functionals, such as the local density approximation (LDA) or the gradient-corrected Perdew-Burke-Ernzerhof (PBE)<sup>23</sup> functional. The gradient-corrected functionals show no binding, whereas the LDA calculations lead to a pronounced minimum with an adsorption

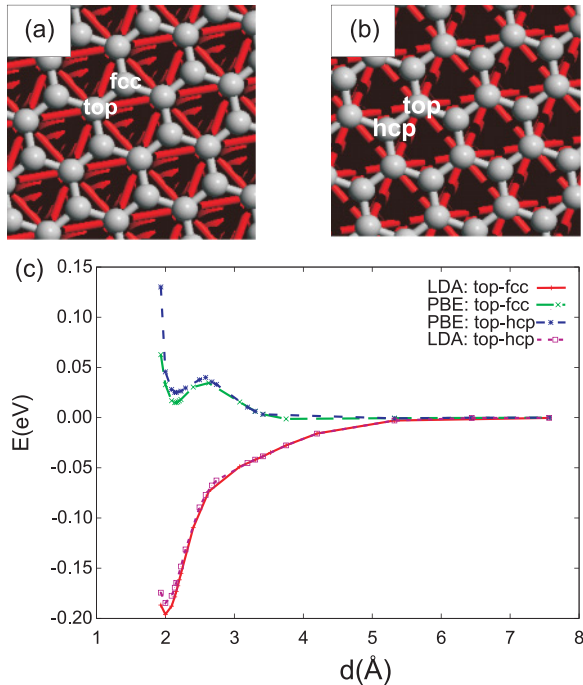


FIG. 1. (Color online) Graphene adsorption on Ni(111) in a top-fcc (a) and top-hcp (b) configuration. (c) DFT adsorption energies vs distance  $d$  calculated with the LDA (red and pink lines) and the PBE exchange-correlation functional (green and blue lines).

energy of 200 meV (using the RPA lattice constant of Ni). For LDA the binding distance of 2.00 Å is closer to the surface than the experimental value of  $2.11 \pm 0.07$  Å,<sup>24</sup> while PBE predicts a local minimum at a correct binding distance of 2.1 Å with an “endothermic adsorption energy” of 15 meV. The weak adsorption energies indicate that the adsorption should not be viewed as a traditional (covalent) chemisorption with typical adsorption energies of 0.5–2 eV. It should also be noted that for semilocal functionals the interaction falls off exponentially and has nothing in common with the correct long-range van der Waals behavior that is expected to be polynomial with distance ( $C_3 \times 1/d^3 - C_4 \times 1/d^4$ ).<sup>25,26</sup> Clearly, both semilocal functionals are missing these van der Waals-like contributions: The deep LDA minimum is a true artifact and is related to the wrong decay of the Kohn-Sham potential and orbitals from the surface into the vacuum.

The bonding at short graphene-Ni distances shows clear signs of a covalent interaction already on the level of semilocal functionals. At a distance  $d = 2.1$  Å, the analysis of the projected band structure of the graphene layer [Fig. 2(a)] shows a pronounced splitting of the  $\pi$  bands (green dots) at the (Dirac)  $K$  point, while the lower-lying  $\sigma$  bands remain unchanged. A similar splitting has been observed for the interaction of graphene with Ru, Rh, and Re surfaces.<sup>27–29</sup> Since the symmetry between the two carbon atoms is lifted, the double degeneracy of the  $\pi$  bands is lifted as well, and two new states appear in the gap at the  $K$  point.

The top site C  $p_z$  orbitals interact strongly with the Ni states (predominantly  $d_{z^2}$ ,  $d_{xz}$ , and  $d_{yz}$ ), leading to strong bonding resonance at  $-2.2$  ( $-1.8$ ) eV for the majority (minority) state at the Dirac points. The hollow site C  $p_z$  also exhibits a

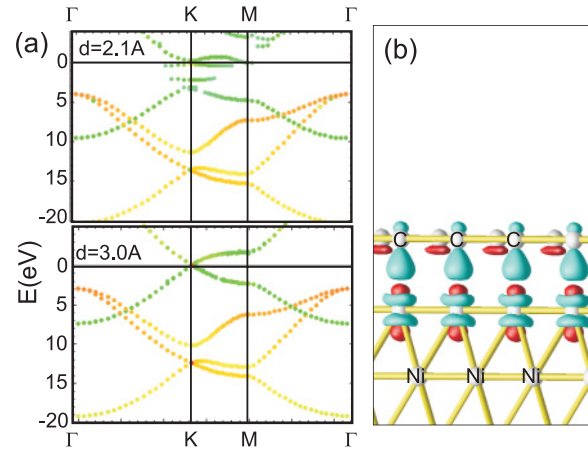


FIG. 2. (Color online) (a) DFT (PBE) band structure of graphene/Ni(111) at a distance of 2.1 and 3 Å projected at the carbon atoms. (b) Differential charge induced by the adsorption of graphene on Ni(111) for a distance of 2.1 Å: The blue/dark gray (red/light gray) areas mark an increase (decrease) of the charge density. No significant changes in the differential charge distribution can be observed at a distance above 3 Å.

resonance with the Ni states, but the interaction energy is, for geometric reasons, weaker and the resonance is located close to the Fermi level at  $-0.5$  ( $+0.1$ ) eV for the majority (minority) states. Antibonding linear combinations are found at energies above the Fermi level. Using a many-electron ( $G_0W_0$ ) approach, only a minor shift of the bonding states to values of  $-2.5$  ( $-1.9$ ) eV for the top C atoms and  $-0.7$  ( $+0.3$ ) eV for the hollow atoms is predicted; the density functional theory predictions are remarkably accurate in this case, although the  $G_0W_0$  values agree best with experiment.<sup>8</sup> The strong resonances are clearly related to the vicinity to the surface, as moving the graphene layer to a larger distance of 3 Å restores the band structure of free-standing graphene with the usual crossing of the  $\pi$  bands at the Fermi level [Fig. 2(a), bottom].

Figure 2(b) shows the differential charge density induced by adsorption. As a result of a strong hybridization between the top-site C  $p_z$  orbital with the Ni  $d_{z^2}$  orbitals, the  $d_{z^2}$  orbitals are partly pushed above the Fermi level, resulting in a depletion of charge in the Ni  $d_{z^2}$  states (graphene-surface antibonding linear combinations), and an increase of the charge density on the C  $p_z$  orbitals (graphene-surface bonding linear combinations at  $-2.0$  eV). Furthermore, we also observe a slight loss of charge from the hollow-site C  $p_z$  orbitals induced by the minority hollow-site C  $p_z$  orbitals being pushed above the Fermi level to  $+0.1$  eV, and an increase of charge on the Ni  $d_{xz}$  and  $d_{yz}$  orbitals. In some respects, the interaction is reminiscent of classical molecule-surface interactions. On the one hand, we have (back)donation from the surface Ni  $d_{z^2}$  states into the top-site C  $p_z$  orbitals, and on the other hand, the hollow-site C  $p_z$  orbitals donate charge to the Ni  $d_{xz}$  and  $d_{yz}$  states. For steric reasons, the second interaction is fairly weak, and we believe that the donation to the surface Ni  $d_{xz}$  and  $d_{yz}$  orbitals is mainly necessitated by the requirement of charge neutrality for the graphene sheet. In fact, a Bader analysis shows that the net charge flow from the surface to graphene is zero. Furthermore, we suspect that the weak hybridization

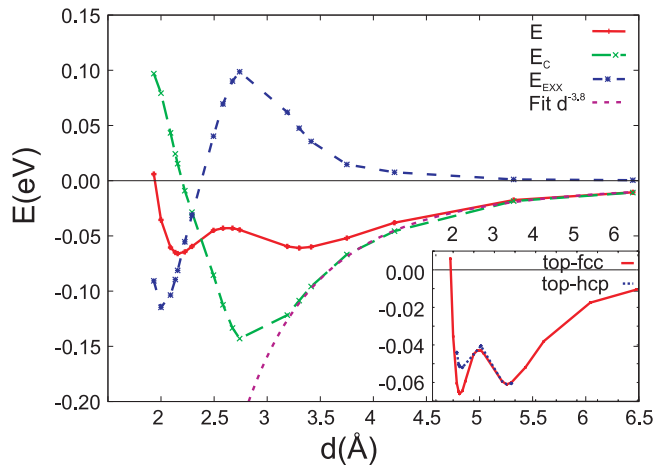


FIG. 3. (Color online) RPA adsorption energies for the adsorption of graphene on Ni(111) in the top-fcc (red/gray line) and top-hcp (inset) configuration. The total adsorption energy is separated into the exchange (blue/dark gray line) and correlation contributions (green/medium gray line). The pink/light gray line indicates an analytic fit to the long-range correlation contributions.

of the hollow-site C atoms with the surface also make the total interaction energies small. The Ni  $d_{xz}$  and  $d_{yz}$  states are pushed to lower energies (below the Fermi surface) as a result of electrostatics related to the loss of charge on the Ni  $d_{z^2}$  states.

To assess the missing nonlocal correlation (van der Waals) contributions, we have explicitly analyzed their contribution in the framework of the RPA. Figure 3 displays the adsorption energy of the graphene sheet in the top-fcc and top-hcp (inset) configurations as a function of the distance to the surface. Evidently, the RPA calculations predict a weak adsorption of the graphene sheet at a distance of 2.17 Å with a binding energy of 67 meV per carbon atom. It should be noted that this value is slightly higher than the calculated binding energy of 48 meV for the graphene sheets in graphite,<sup>17</sup> indicating that the graphene sheet will wet the surface, in agreement with experiment.

Interestingly, the RPA calculations do not only predict one single minimum but also a second minimum at a distance of 3.3 Å. This second minimum, which is slightly weaker bound with an adsorption energy of 60 meV, is at typical distances for van der Waals adsorbed graphene on transition metals.<sup>6</sup> The breakup of the exchange and correlation contributions to the energy and the previously shown band structures hint at the origin of this behavior. At large distances, up to 2.8 Å, the band structure of graphene is hardly modified, the exchange interaction is purely repulsive, and the correlation follows essentially a vdW-like behavior: The long-range contributions of the correlation energy can be fitted well by a curve following  $d^{-3.84}$  (Fig. 3, pink/light gray line). The value of the exponential is rather close to  $-4$ , indicative of a simple additive pairwise interaction between two sheets.<sup>17</sup> We note that this behavior might change qualitatively at very large distances,<sup>17,26</sup> but at the intermediate distances considered here, a pairwise interaction seems to describe the overall behavior rather well.

At distances shorter than 2.8 Å, the graphene band structure starts to be modified with a hybridization setting in, and most importantly, with a breakup of symmetry between the top-site C atoms and hollow-site C atoms. For the related adsorption of graphene on Ir(111), a small hybridization has been predicted even for a slightly larger distance of 3.2 Å, presumably due to the less localized Ir  $5d$  states.<sup>30</sup> The symmetry reduction and the hybridization abruptly change the exchange energy, resulting in a strong interaction even on the level of exact exchange (EXX). Part of the reason for this decrease of the exchange energy is that Hartree-Fock prefers a symmetry-broken solution for the free-standing graphene layer, i.e., an insulating charge wave ground state with disproportionated carbon atoms is preferred over the metallic ground state. Such a charge wave is induced by the metal slab, lowering the EXX energy. Correlation, however, restores the correct nonsymmetry-broken ground state for free-standing graphene, and concomitantly on the surface, the correlation rises almost as steeply as the exchange energy decreases. The resulting total energy is smooth, with a slight barrier between the physisorption minimum, characterized by a graphene band structure that is hardly modified compared to free-standing graphene, and the second “chemisorption” minimum, where the graphene band structure is strongly modified compared to the free-standing layer.

To complete our RPA studies, we also considered adsorption with the carbon atoms at the top and hcp sites. The curve is virtually identical to the top-fcc curve at larger distances up to the first physisorption minimum where vdW interactions dominate. Only at the closer distances does the top-fcc configuration gain stability over the top-hcp configuration, which yields only an adsorption energy of 52 meV.

Finally, we want to address the question as to whether the computationally rather demanding RPA results can be reproduced with a less involved method. Although the van der Waals DFT (vdW-DF)<sup>13</sup> might seem to be a promising candidate, it was recently shown that the original functionals were too repulsive at short distances.<sup>14</sup> The strong repulsion can be alleviated by another choice for the semilocal exchange-correlation functional.<sup>31</sup> Figure 4 gives an overview on the

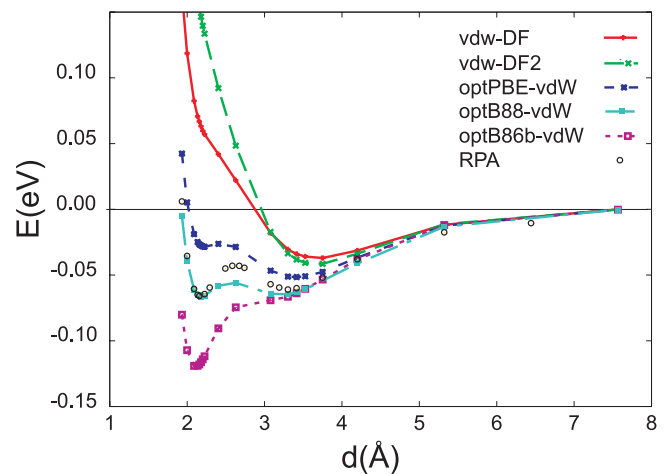


FIG. 4. (Color online) Adsorption of graphene (top fcc) on Ni(111) using the vdW DFT as a function of the exchange-correlation functional.

predictions of various flavors of the vdW-DF. The comparison clearly shows that the results from the vdW-DF calculation strongly depend on the actual flavor of the vdW functional. While the originally proposed vdW-DF and vdW-DF2 still result in nonbonding behavior in the vicinity of the surface, the vdW functionals (“opt”) recently developed by Klimeš and Michaelides<sup>31,32</sup> lead to improved binding at short distances. It should be noted that especially the results obtained with the optB88-vdW functional are in good agreement with the RPA data, with the binding energy at the two minima (67 and 65 meV) very close to the RPA values. This agreement can be, to some extent, coincidental and studies on other substrates should be performed to see if it is a general feature.

Summarizing, we have evaluated the interaction of a graphene layer with a ferromagnetic Ni(111) substrate. The most remarkable result is the presence of two minima, one at typical physisorption distances of 3.3 Å, and a second one at shorter distances of 2.17 Å. Our analysis indicates that the common concepts of adsorption cannot be applied to this system, as we observe both strong signs of chemisorption

at these short distances, but also an adsorption energy that remains in the typical range of weak physisorption. We believe that this is related to the lack of an efficient hybridization mechanism for donation of charge from the carbon overlayer to the surface, for instance, via the hollow-site carbon  $p_z$  orbitals. Using our accurate data for the energy-distance curve allows us to assess the quality of the computationally significantly cheaper vdW-DF functionals. Especially, the good agreement between the optB88-vdW results and the RPA calculations make this vdW functional a promising choice for the treatment of larger systems where the graphene-metal interaction has to be described accurately. Thus our study presents an important step for the theoretical understanding of graphene-based electronics.

This work has been supported by the European Science Foundation (ESF) under the EUROCORES project EUROGRAPHENE/SpinGraph and the Austrian Science Fund (FWF) under Grants I422-N16 and the SFB ViCoM. The Vienna Scientific Cluster (VSC) is acknowledged for CPU time.

\*fmi@cms.tuwien.ac.at

<sup>1</sup>A. K. Geim, *Science* **324**, 1530 (2009).

<sup>2</sup>A. K. Geim and K. S. Novoselov, *Nat. Mater.* **6**, 183 (2007).

<sup>3</sup>F. Schwierz, *Nat. Nanotechnol.* **5**, 487 (2010).

<sup>4</sup>V. M. Karpan, P. A. Khomyakov, A. A. Starikov, G. Giovannetti, M. Zwierzycki, M. Talanana, G. Brocks, J. van den Brink, and P. J. Kelly, *Phys. Rev. B* **78**, 195419 (2008).

<sup>5</sup>J. Winterlin and M.-L. Bocquet, *Surf. Sci.* **603**, 1841 (2009).

<sup>6</sup>P. Sutter, J. T. Sadowski, and E. Sutter, *Phys. Rev. B* **80**, 245411 (2009).

<sup>7</sup>A. Grüneis and D. V. Vyalikh, *Phys. Rev. B* **77**, 193401 (2008).

<sup>8</sup>Yu. S. Dedkov and M. Fonin, *New J. Phys.* **12**, 125004 (2010).

<sup>9</sup>G. Bertoni, L. Calmels, A. Altibelli, and V. Serin, *Phys. Rev. B* **71**, 075402 (2005).

<sup>10</sup>G. Kalibaeva, R. Vuilleumier, S. Melvoni, A. Alavi, G. Cicotti, and R. J. Rosei, *Phys. Chem. B* **110**, 3638 (2006).

<sup>11</sup>G. Giovannetti, P. A. Khomyakov, G. Brocks, V. M. Karpan, J. van den Brink, and P. J. Kelly, *Phys. Rev. Lett.* **101**, 026803 (2008).

<sup>12</sup>M. Fuentes-Cabrera, M. I. Baskes, A. V. Melechko, and M. L. Simpson, *Phys. Rev. B* **77**, 035405 (2008).

<sup>13</sup>M. Dion, H. Rydberg, E. Schroder, D. C. Langreth, and B. I. Lundqvist, *Phys. Rev. Lett.* **92**, 246401 (2004).

<sup>14</sup>I. Hamada and M. Otani, *Phys. Rev. B* **82**, 153412 (2010).

<sup>15</sup>J. Harl and G. Kresse, *Phys. Rev. Lett.* **103**, 056401 (2009).

<sup>16</sup>H. Eshuis and F. Furche, *J. Phys. Chem. Lett.* **2**, 983 (2011).

<sup>17</sup>S. Lebegue, J. Harl, T. Gould, J. G. Angyan, G. Kresse, and J. F. Dobson, *Phys. Rev. Lett.* **105**, 196401 (2010).

<sup>18</sup>L. Schimka, J. Harl, A. Stroppa, A. Grüneis, M. Marsman, F. Mittendorfer, and G. Kresse, *Nat. Mater.* **9**, 741 (2010).

<sup>19</sup>G. Kresse and J. Hafner, *Phys. Rev. B* **47**, 558 (1993).

<sup>20</sup>G. Kresse and J. Furthmüller, *J. Comput. Mater. Sci.* **6**, 15 (1996).

<sup>21</sup>G. Kresse and D. Joubert, *Phys. Rev. B* **59**, 1758 (1999).

<sup>22</sup>J. Harl, L. Schimka, and G. Kresse, *Phys. Rev. B* **81**, 115126 (2010).

<sup>23</sup>J. P. Perdew, K. Burke, and M. Ernzerhof, *Phys. Rev. Lett.* **77**, 3865 (1996).

<sup>24</sup>Y. Gamo, A. Nagashima, M. Wakabayashi, M. Terai, and C. Oshima, *Surf. Sci.* **374**, 61 (1997).

<sup>25</sup>J. L. F. Da Silva, C. Stampfl, and M. Scheffler, *Phys. Rev. Lett.* **90**, 066104 (2003).

<sup>26</sup>J. F. Dobson, A. White, and A. Rubio, *Phys. Rev. Lett.* **96**, 073201 (2006).

<sup>27</sup>S. J. Altenburg, J. Kröger, B. Wang, M.-L. Bocquet, N. Lorente, and R. Berndt, *Phys. Rev. Lett.* **105**, 236101 (2010).

<sup>28</sup>A. B. Preobrajenski, M. L. Ng, A. S. Vinogradov, and N. Mårtensson, *Phys. Rev. B* **78**, 073401 (2008).

<sup>29</sup>S. Marchini, S. Günther, and J. Winterlin, *Phys. Rev. B* **76**, 075429 (2007).

<sup>30</sup>C. Busse *et al.*, *Phys. Rev. Lett.* **107**, 036101 (2011).

<sup>31</sup>J. Klimeš, D. R. Bowler, and A. Michaelides, *Phys. Rev. B* **83**, 195131 (2011).

<sup>32</sup>J. Klimeš, D. R. Bowler, and A. Michaelides, *J. Phys. Condens. Matter* **22**, 022201 (2010).